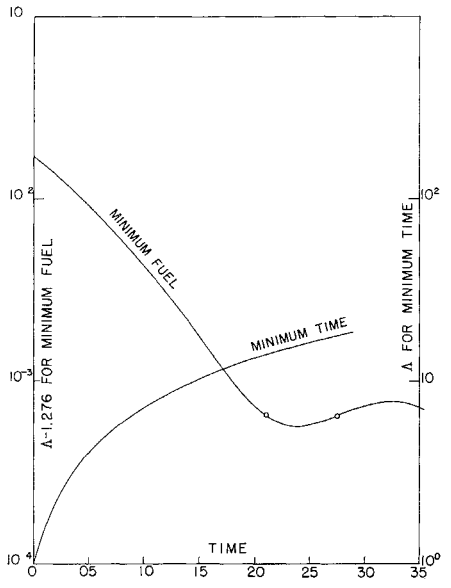

Fig 2 Λ vs time

modify the $[\dot{U},\dot{V},U,V,X,Y]_T$ terms in the Newton-Raphson equations before solving these equations, so as to minimize the sum of the squares of the elements of $[U - u, V - v, X - x, Y - y]_T$

The numerical example of minimum fuel transfer given here involves the same launching conditions, mass loss parameters, and circular orbit used in the minimum time transfer of Ref 1 The results for minimum fuel transfer are $T = 0\,353977$, $t_1 = 0\,210293$, $t_2 = 0\,275349$, $l = -0\,820196$, $m = -0\,708727$, $n = -1\,181390$, and the transfer sector angle $B = 0\,189345$ rad Since the minimum time trajectory of Ref 1 gave $T = 0\,289869$, the net fuel saving in minimum fuel transfer over minimum time transfer is measured by $0\,289869 - 0\,353977 + t_2 - t_1 = 0\,000948$, or an unspectacular $\frac{1}{3}\%$ Figure 1 shows the trajectories and thrust directions for minimum time and minimum fuel transfer

The semilogarithmic plots of Fig 2 show the different behavior of Λ vs time in the two problems For some reason there is a much greater difference than expected The curve increases monotonically for minimum time transfer The curve for minimum fuel shows a rather characteristic shape It is initially large and decreasing; it then increases, and then decreases If the final decreasing interval does not occur, larger values of T lead to lower values of fuel consumption, as may be partially inferred from Eq (7)

Reference

[1] Bleick, W E, "Orbital transfer in minimum time," AIAA J 1, 1229–1231 (1963)

Hypersonic Blunt-Body Flow Fields at Angle of Attack

RUDOLPH J SWIGART*
Lockheed Missiles and Space Company, Huntsville, Ala

I Introduction

A NEW method of solving the supersonic blunt-body problem has been developed recently by the author [1] This method has proved to be as accurate as other methods in popular use for calculating plane-symmetric and axisymmetric flow in the subsonic portion of the shock layer, and has the additional advantage of being readily extendable to the calculation of flows about blunt-nosed configurations at angle of attack

The method is an inverse one, that is, the freestream conditions and shape of the detached shock wave are taken as known, and the body shape and flow field are to be determined The success of the method rests with the rapid convergence of assumed power-series expansions for certain flow variables about the shock-wave axis of symmetry and about zero angle of attack Only first order terms in angle of attack are retained Substitution of these series into the governing differential equations and boundary conditions reduces the problem to integration of ordinary differential equations that determine the series coefficients The integration can be performed by truncating the series about the shock-wave axis of symmetry at any desired number of terms

Reference 1 contains results for flow past inclined blunt bodies for two shock-wave shapes at infinite freestream Mach numbers In that report, attention is focused on the question of whether or not the streamline that wets the body in asymmetric flow is the one that crosses the shock at right angles and hence has maximum entropy in the shock layer It is pointed out that, in a properly posed method of analysis, no assumption regarding the behavior of the maximum-entropy streamline is required Consideration of flow past bodies supporting parabolic (two-dimensional) and paraboloidal (three-dimensional) shock waves at positive angle of attack leads to the conclusion that the maximum-entropy and body streamlines are not one and the same, the maximum-entropy streamline passing slightly below the body in both cases In Part I of Ref 1, prior solutions to the asymmetric problem by other investigators are discussed, and it is noted that these solutions depend upon the assumption that the body is wetted by the streamline of maximum entropy Indeed, even in work published more recently than Ref 1, this assumption is still being made [2]

Subsequent to the work described in Ref 1, the algebra involved has been carried out for obtaining results from the theory of that reference for inclined bodies of arbitrary shape (with the not too confining restriction that these bodies support shock waves that are conic sections) at arbitrary freestream Mach number Two computer programs have been developed, one to calculate asymmetric flow past inclined two-dimensional bodies, and the other to handle three-dimensional flow past inclined bodies supporting axisymmetric shock waves

Several results of these computer programs are presented in this note A critical appraisal is made of the error involved in neglecting second and higher-order terms in the angle-of-attack series by considering flow past circular and spherical shock waves at freestream Mach numbers of infinity and 4 0 Since the flow past a circular or spherical shock wave at angle should be the same as the flow past these same shock waves at zero angle and rotated through the angle of attack, comparison with rotated zero-angle solutions provides an index of the error generated by neglecting higher-order terms Flow past a 3:2 axis-ratio prolate ellipsoid of revolution at 7 5° angle of attack is also considered, and results for the surface pressure distribution in the vertical symmetry plane are compared with the experiment

II Analysis

The details of analysis of asymmetric blunt-body flows by the method of series expansion about the shock-wave axis of symmetry and about zero angle of attack are given in Ref 1 Equations (8a, 8b, 9a, 10a, and 11) of that report govern two-dimensional asymmetric flow The boundary conditions at the shock wave and explicit expression for the function $f(\psi)$ [Eqs (9a) and (10a) of Ref 1], are derived in Appendix I of Ref 3 The differential equations governing

Received September 19, 1963
* Head Theoretical Fluid Mechanics Research

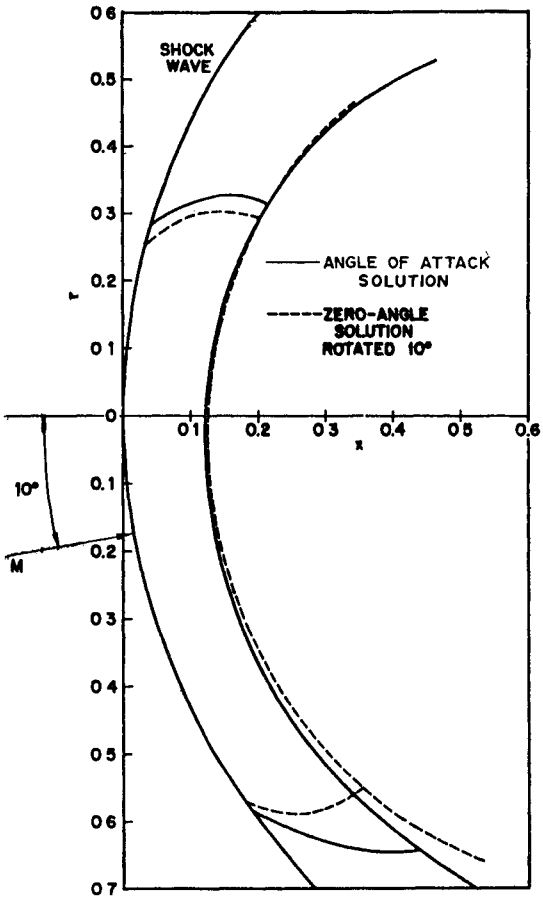

Fig 1 Body shapes and sonic lines; spherical shock, M = 4 0, γ = 1 4, ϵ = 10°

three-dimensional flow are Eqs (24a–24c) of Ref 1 However, two of the three-dimensional boundary conditions at the shock wave, namely, Eqs (25d) and (25e) of Ref 1, are incorrect The correct forms of these equations are derived in Appendix II of Ref 3, along with the other three-dimensional boundary conditions and the explicit expression for the function $g(\psi_1,\psi_2)$ Hence, the complete set of equations governing three-dimensional flow in the shock layer are Eqs (24a–24c, 25a–25c, 26a, and 27) of Ref 1, along with Eqs (36) and (37) of Appendix II of Ref 3 Equations (12a) and (12b) of Ref 1 give the assumed form of the series for the stream function and density for the two-dimensional case, and Eqs (28a–28c) give corresponding forms for the three-dimensional case

For the solutions investigated in this report, the expansions about the shock-wave axis of symmetry are truncated at three terms (counting nonzero terms only), and only first-order terms in the expansions about zero angle of attack are retained For example, the series for the two-dimensional stream function in orthogonal curvilinear coordinates (ξ,η) in which the shock wave is a constant coordinate surface defined by $\eta = 1$ (see Ref 1) takes the form,

$$\psi = f_{00}(\eta) + f_{01}(\eta)\xi^3 + f_{02}(\eta)\xi^5 + \epsilon[f_{10}(\eta) + f_{11}(\eta)\xi^2 + f_{12}(\eta)\xi^4]$$

where $\xi = 0$ defines that portion of the shock-wave axis of symmetry of interest, and ϵ is the shock-wave angle of attack

III Results and Discussion

As a means of assessing the error due to retention of only first-order terms in angle of attack in the series expansions for the stream functions and density, the flow past bodies supporting spherical and circular shock waves at 10° angle

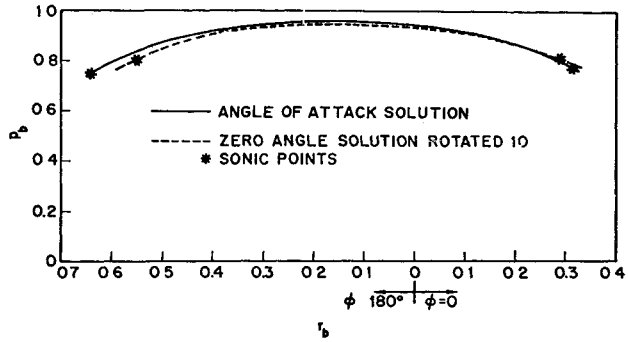

Fig 2 Surface pressure distribution; spherical shock, M = 4 0, γ = 1 4, ϵ = 10°

of incidence was considered Since the flow past a body supporting a spherical or circular shock at incidence should be identically the flow at zero angle rotated through the angle of attack, comparison of the incident and rotated zero-angle solutions gives an indication of the error introduced in neglecting second- and higher-order terms in shock-wave angle of attack Strictly speaking, the error due to neglect of higher-order terms in angle of attack cannot be separated from that due to truncation of the series about the shock-wave axis of symmetry However, since previous investigations[1] at zero angle of attack have shown body shape and sonic line position to be nearly converged when three terms in the series about the shock-wave axis of symmetry are retained, the truncation error is considered small with respect to that, due to neglect of higher-order terms in angle of attack

Figures 1 and 2 compare results of the angle-of-attack and rotated zero-angle solutions for flow past the body supporting a spherical shock wave at freestream Mach number, M, of 4 0 Figure 1 shows that body shape and sonic line agreement is good in the upper half ($\varphi = 0°$) plane, but only fair in the lower half ($\varphi = 180°$) plane However, Fig 2 shows excellent agreement of the surface-pressure distributions, the small error being on the high side over most of the region of interest This error is due to neglect of higher-order terms in angle of attack, and the fact that the angle-of-attack solution yields high values for the surface pressure may be concluded by considering the series expansion for the surface pressure,

$$p_b = p_0(\xi,\eta_b) + \epsilon p_1(\xi,\eta_b) + 0(\epsilon^2) \quad (1)$$

where $p_0(\xi,\eta_b)$ is the surface-pressuie distribution at zero angle of attack, and $\epsilon p_1(\xi,\eta_b)$ is the first order correction due to angle of attack Now, $p_0(\xi,\eta_b)$ may be further expanded in an even series in ξ,

$$p_0(\xi,\eta_b) = p_{00}(\eta_b) + p_{01}(\eta_b)\xi^2 + p_{02}(\eta_b)\xi^4 + 0(\xi^6) \quad (2)$$

whereas $p_1(\xi,\eta_b)$ may be expanded in an odd series in ξ,

$$p_1(\xi,\eta_b) = p_{10}(\eta_b) + p_{11}(\eta_b)\xi^3 + p_{12}(\eta_b)\xi^5 + 0(\xi^7) \quad (3)$$

Thus, at $\xi = 0$, $p_b = p_{00}(\eta_b) + 0(\epsilon^2)$ Hence, to first order in ϵ, $p_b = p_{00}(\eta_b)$ at $\xi = 0$ regardless of the value of ϵ At zero angle of attack, $p_{00}(\eta_b)$ is the stagnation-point pressure At angle of attack, however, the stagnation point is not in the same place as at zero angle, and the pressure at the angle-of-attack stagnation point must necessarily be higher than at $\xi = 0$ Thus the pressure increases as one moves from $\xi = 0$ to the angle-of-attack stagnation point, resulting in consistently high pressure values along the body in the region of interest Figure 2 corroborates these conclusions Note that the pressure at $r_b = 0(\xi = 0)$ for the angle-of-attack solution (solid line) is precisely the same as the stagnation-point pressure of the zero-angle solution rotated 10° (dotted line), the stagnation point being at $r_b = 0\ 152$ in the $\varphi = 180°$ plane

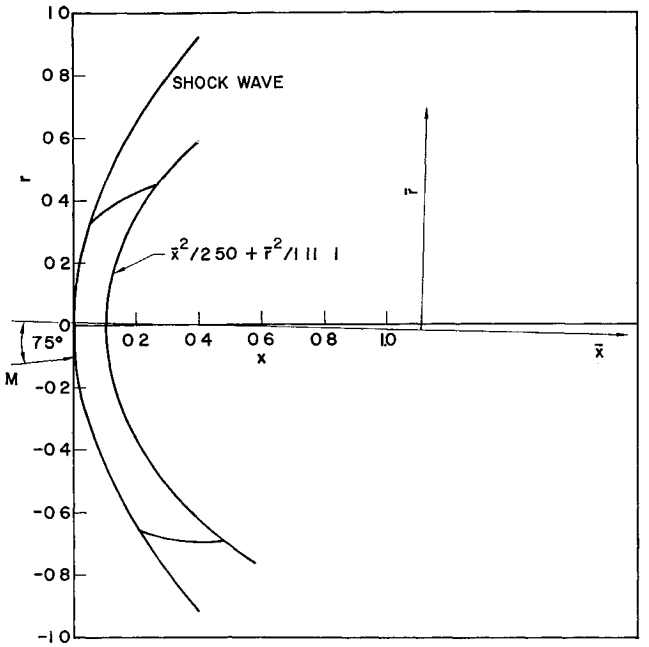

Fig 3 Body shape and sonic lines; 3:2 prolate ellipsoid of revolution, $M = 8.08$, $\gamma = 1.4$, $\epsilon = 6°$, $\alpha = 7.5°$

For a discussion of similar comparisons for flow past the body supporting a spherical shock at infinite freestream Mach number, and for flow past two-dimensional bodies supporting circular shock waves at freestream Mach numbers of infinity and 4.0, see Ref. 3. In general, body-shape agreement is good in the two-dimensional cases. Agreement of sonic-line positions and surface-pressure distributions, however, is only fair, being slightly poorer than the corresponding three-dimensional cases.

Figure 3 shows the profile in the vertical symmetry plane of a body having the same cross section in this plane as a 3-to-2 axis ratio prolate ellipsoid of revolution at 7.5° angle of attack. The body supports the shock wave shown at a freestream Mach number of 8.08. This Mach number was chosen in order that experimental results for the surface pressure distribution on a 3-to-2 prolate ellipsoid of revolution at 7.5° angle of attack could be compared with those of theory. The comparison is made in Fig. 4. Note that agreement between the theoretical curve and experimental data is excellent. In light of the previously discussed systematically high surface-pressure distributions predicted by theory, one must conclude that the error is small for this case (cf. Fig. 2). Note that the angle-of-attack of the body α is 7.5°. This corresponds to a shock-wave angle of attack ϵ of 6°. Hence, the reduction in ϵ^2 over the previously considered data is 64%, which aids significantly in reducing the error in the surface-pressure distribution.

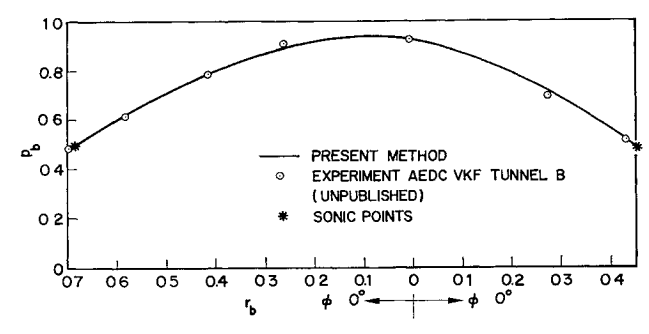

Fig 4 Surface pressure distribution; 3:2 prolate ellipsoid of revolution, $M = 8.08$, $\gamma = 1.4$, $\epsilon = 6°$, $\alpha = 7.5°$

References

[1] Swigart, R. J., "A theory of asymmetric hypersonic blunt-body flows," IAS Preprint 62-98 (June 1962).

[2] Vaglio Laurin, R., "Inviscid supersonic flow about general three dimensional blunt bodies," TR ASD-TR 61-727, Vol. I, Flight Dynamics Lab., Aeronaut. Systems Div., Air Force Systems Command, Wright Patterson Air Force Base, Ohio (October 1962).

[3] Swigart, R. J., "Hypersonic blunt-body flow fields at angle of attack," Fluid Mech. Res. Rept. 5, Mech. and Math. Sci. Lab., Lockheed Missiles and Space Co., Palo Alto, Calif. (May 1963).

Determination of Propellant Properties by the Arc Image Furnace Technique

R. O. Fleming, Jr.* and R. W. Fleming†

Bermite Powder Company, Saugus, Calif.

THE arc image furnace technique[1] has been used for the past several years for the determination of threshold ignition energies (q) of propellants and igniter materials. The particular arc image design used in these studies consists of opposed ellipsoids with a shuttering mechanism at the common minor focus. A high intensity carbon arc located at the major focus of one ellipsoid is imaged on the sample surface located at the major focus of the other ellipsoid (see Fig. 1). The samples, which are about 8 mm in diameter by about 5 mm thick, are located precisely within a cylindrical cast acrylic firing chamber whose volume is about 125 cm^3. The chamber can be subjected to varying environmental conditions of pressure, temperature, and flow.

An Elastronics, Inc.,‡ type TR 4001 radiation transducer is located at one end of the firing chamber so that it views the sample surface to be irradiated. The transducer consists of a germanium photo transistor located behind a sapphire "light pipe" and is capable of producing temperature vs time profiles by means of an oscilloscope and recording camera.

In practice, the firing chamber is connected to a surge tank whose volume is about 12,500 cm^3. The material to be tested is either cut (in the case of the solid propellants) or press-loaded in suitable retaining rings (in the case of igniter materials). Sample thickness is determined micrometrically. The rear surface of each sample is spotted with a drop of bead mix which contains a high percentage of zirconium. Each sample is then exposed to a predetermined amount of energy and "go/no go" data is obtained so that the Bruceton or

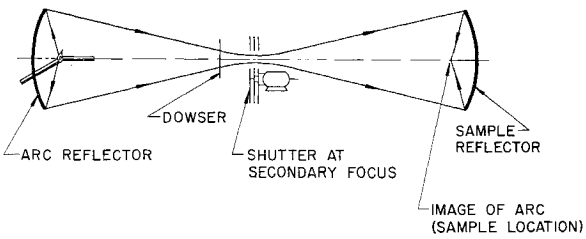

Fig 1 Schematic drawing of double ellipsoidal mirror system

Received September 18, 1963. The work described in this technical note was supported by the U. S. Navy, Bureau of Weapons, Contract NOw 62-0236-c.

* Manager, Research Group, Research and Development Division.

† Engineer, Research Group, Research and Development Division.

‡ Elastronics Inc., 19458 Ventura Blvd., Tarzana, Calif.